Proceedings of the 20th International Conference on Soil Mechanics and Geotechnical Engineering– Rahman and Jaksa (Eds)

A simple method to verify soil model implementation by observing the performance on π plane

Mettre en œuvre une nouvelle méthode simple pour vérifier la mise en œuvre d'un modèle de sol en observant les performances en vol

Zhichao Wang & Yun Qin
Hunan Key Laboratory of Geomechanics and Engineering Safety & College of Civil Engineering and Mechanics, Xiangtan University, Xiangtan, Hunan 411105, China, wzc@xtu.edu.cn

Yinghui Tian
Department of Infrastructure Engineering, The University of Melbourne, Victoria, 3010 Australia

ABSTRACT: Numerical implementation of soil constitutive models is a challenging task, where a fundamental and critical step is the verification of the numerical code by observing the preformation by showing the yield surface on the π plane and other specified stress paths. Unfortunately, this remains as difficult work as most of the currently available programs did not directly provide this functionality. This paper provides a simple methodology to realize this based on the commercial package, ABAQUS. User Subroutine URDFIL is used to extract the element stress and strain information and Subroutine DLOAD is used to control the load (stress) according to the required stress path. The data exchange between the two User Subroutines is realized by two Utility Subroutines, POSFIL, and DBFILE. A 'release spring' is introduced to ensure that the complete data can be obtained during the analysis. This method has been tested by using Mohr-Coulomb model, Matsuoka-Nakai model, Lade-Duncan model, Drucker-Prager model, and an elasto-viscoplastic model based on super-subloading yield surface, respectively. The model preformation with constant mean effective stress, i.e. on the π plane is observed. The results show: 1) the failure curve on the π plane of the principal stress space can be correctly obtained by the proposed method, and the shape is consistent with the theoretical results of the above models; 2) the method has shown a stable convergence and high precision; 3) the method provides a practical way for verifying strain hardening, strain softening, elastoplastic, elasto-viscoplastic, and other complex models.

RÉSUMÉ : La mise en œuvre numérique de modèles constitutifs du sol est une tâche difficile, où une étape fondamentale et critique est la vérification du code numérique en observant la préformation en montrant la surface de rendement sur le plan du module et d'autres trajectoires de contraintes spécifiées. Malheureusement, cela reste aussi difficile que la plupart des programmes actuellement disponibles ne fournissent pas directement cette fonctionnalité. Le présent document fournit une méthodologie simple pour réaliser cet objectif, basée sur le progiciel commercial ABAQUS. Le sous-programme utilisateur URDFIL est utilisé pour extraire l'information sur les contraintes et les déformations des éléments et le sous-programme DLOAD est utilisé pour contrôler la charge (contrainte) en fonction du chemin de contrainte requis. L'échange de données entre les deux sous-programmes utilisateurs est réalisé par deux sous-programmes utilitaires, POSFIL et DBFILE. Un «ressort de libération» est introduit pour garantir que les données complètes peuvent être obtenues au cours de l'analyse. Cette méthode a été testée en utilisant respectivement le modèle de Mohr-Coulomb, le modèle de Matsuoka-Nakai, le modèle de Lade-Duncan, le modèle de Drucker-Prager et un modèle élasto-viscoplastique basé sur la supersous-charge de surface de rendement. On observe la préformation du modèle avec une contrainte effective moyenne constante, c'est-à-dire sur le plan droit. Les résultats montrent: 2) la méthode a montré une convergence stable et une grande précision; 3) la méthode fournit un moyen pratique de vérifier l'écrouissage, l'adoucissement, l'élastoplastique, l'élasto-viscoplastique et d'autres modèles complexes.

KEYWORDS: Numerical implementation; stress path; constant mean effective stress; π plane; strain softening.

1 INTRODUCTION

Soil constitutive models (such as Hashiguchi et al.,1998; Wheeler et al., 2003; Tasiopoulou et al., 2016) with different yield criteria are employed to characterize experimental observation. The shape of classical yield criteria such as Tresca, von Mises, Drucker-Prager, Mohr-Coulomb, Matsuoka-Nakai, and Lade–Duncan on the π plane (namely, the deviatoric section) has been well defined (Lagioia et al., 2016), especially with the envelope of yield locus on the π plane. Experimentally, true triaxial tests and triaxial constant mean principal stress tests can be carried out to observe and obtain the yield locus of soil constitutive model on the π plane by showing the shear behavior of soil samples along the loading paths of different Lodes angles, such as Nakai (1986). Unfortunately and surprisingly, carrying out this numerical constant mean effective stress triaxial test and thus verifying the yield surface on the π plane does not seem to be straightforward work in most of the currently available programs of finite element package. This paper provides a simple methodology to realize this by showing the yield surface on the π plane and other any specified stress paths, based on the commercial package, ABAQUS.

This is demonstrated by showing a finite element model to simulate triaxial constant mean effective stress test, where User Subroutine URDFIL is used to extract the element stress and strain information and Subroutine DLOAD is used to control the load (stress) according to the required stress path. The yield locus of any soil constitutive model can thus be observed on the π plane.

2 SIMULATION OF TRUE TRIAXIAL CONSTANT MEAN EFFECTIVE STRESS TEST

2.1 *Basic concept of the π plane*

The stress-strain relationship of soil can be described by the principal stresses σ_1, σ_2, and σ_3 ($\sigma_1 \geq \sigma_2 \geq \sigma_3$) in the principal stress space as shown in Figure 1.

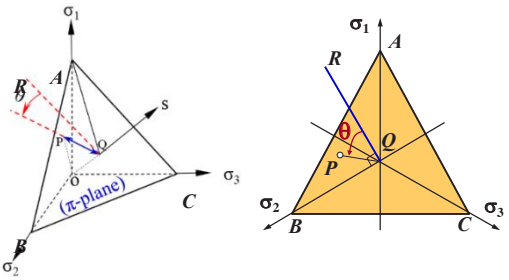

(a) Spatial graphic (b) Planar projection

Figure 1. Schematic diagram of the deviatoric section (π-plane) in the principal stress space.

The point P in this space represents a stress state, and the line OP represents a stress path, where the π plane is defined as a special plane perpendicular to the trisectrix OS in the principal stress space. The angle between line QP and QR is defined as Lode's angle θ, and it is agreed to be positive with counter-clockwise rotation from line QP to QR. The modules of lines PQ and OQ, as well as Lode's angle θ of the stress state point P, can also be given as follow:

$$|\mathrm{OQ}| = \frac{1}{\sqrt{3}}(\sigma_1+\sigma_2+\sigma_3) = \sqrt{3}I_1 \tag{1}$$

$$|\mathrm{PQ}| = \frac{\sqrt{(\sigma_1-\sigma_2)^2+(\sigma_2-\sigma_3)^2+(\sigma_3-\sigma_1)^2}}{\sqrt{3}} = \sqrt{2J_2} = \sqrt{\frac{2}{3}}q \tag{2}$$

$$\mathrm{tg}\theta = \frac{2\sigma_2-\sigma_1-\sigma_3}{\sqrt{3}(\sigma_1-\sigma_3)} = \frac{\mu_\sigma}{\sqrt{3}} \tag{3}$$

Where I_1 is the first invariants of the effective stress tensor; J_2 is the second invariant of the deviatoric stress tensor; q is the deviatoric stress; μ_σ is the Lode's coefficient.

2.2 *Specified stress paths of constant mean effective stress*

To determine the yield locus of the soil sample on the π plane, a true triaxial constant mean effective stress test needs to be performed along a specified stress path as seen in Figure 2.

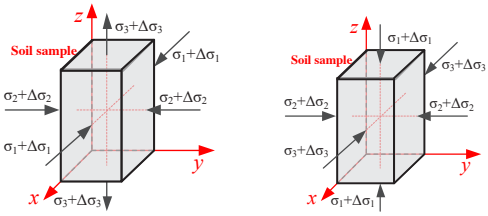

(a) Triaxial tension (b) Triaxial compression

Figure 2. Loading schematic diagram of true triaxial element test along the specified stress paths

Firstly, the soil sample is isotopically consolidated to the mean effective stress σ_m, namely

$$\sigma_1=\sigma_2=\sigma_3=\sigma_m \tag{4}$$

Secondly, under the condition that the mean effective stress σ_m remains unchanged, the soil samples are subjected to triaxial tension or triaxial compression along the specified loading stress path. The increment sizes of the three principal stresses must meet the following equation

$$\Delta\sigma_1+\Delta\sigma_2+\Delta\sigma_3=0 \tag{5}$$

During the triaxial tension

$$\begin{cases}\Delta\sigma_1=B_1\cdot\Delta\sigma_3\\ \Delta\sigma_2=B_2\cdot\Delta\sigma_3\end{cases} \text{ or } \begin{cases}\Delta\sigma_x=B_1\cdot\Delta\sigma_z\\ \Delta\sigma_y=B_2\cdot\Delta\sigma_z\end{cases} \tag{6}$$

During the triaxial compression

$$\begin{cases}\Delta\sigma_3=B_1\cdot\Delta\sigma_1\\ \Delta\sigma_2=B_2\cdot\Delta\sigma_1\end{cases} \text{ or } \begin{cases}\Delta\sigma_x=B_1\cdot\Delta\sigma_z\\ \Delta\sigma_y=B_2\cdot\Delta\sigma_z\end{cases} \tag{7}$$

Substitute Eq. (6) or (7) into Eq. (5), It can be found that $B_1+B_2=-1$ on the conditions of both triaxial tension and triaxial compression. Once the values of B_1 and B_2 are determined, Lode's angle θ can be calculated according to Eq. (3) combined with Eq. (6) or (7), and the relationship among Lode's angle θ, B_1, and B_2 along the specified loading stress paths is given in Table 1.

Table 1. Relationship among Lode's angle θ, B_1 and B_2 along the specified loading stress paths

Lode's angle θ		B_1	B_2
Tension	Compression		
30	-30	-0.5	-0.5
25	-25	-0.575767405	-0.424232595
20	-20	-0.652703645	-0.347296355
15	-15	-0.732050808	-0.267949192
10	-10	-0.815207469	-0.184792531
5	-5	-0.903834278	-0.096165722
0	0	-1	0

Table 1 shows that the confining pressure increment $\Delta\sigma_2$ and $\Delta\sigma_3$ decreases as the axial stress increment $\Delta\sigma_1$ increases during triaxial compression, but the confining pressure increment $\Delta\sigma_1$ and $\Delta\sigma_2$ increases as the axial stress increment $\Delta\sigma_3$ decreases during triaxial tension. When the deviatoric stress q of the soil sample reaches its yield strength in the triaxial compression (or tension), the axial stress increment $\Delta\sigma_z=0$. It's challenging for the soil element to be further loaded and deformed after its deviatoric stress reaches its yield strength.

2.3 *Numerical implementation of the triaxial constant mean effective stress test*

To overcome the above problem, a so-called slow-release spring is employed to balance the axial stress increment after the deviatoric stress of the soil sample reaches its yield strength, as shown in Figure 3. The elastic coefficient of the slow-release spring is E_s, and its length is h. The length of the soil sample is H. During the triaxial compression (or tension) with constant mean effective stress, the surface $EFGH$ is fixed and the surface $EFGH$ under loading stress P_z can be moved down (or up) along the z-axis, where this displacement is defined as u_z, and its positive direction is the same as the positive direction of the coordinate axes z.

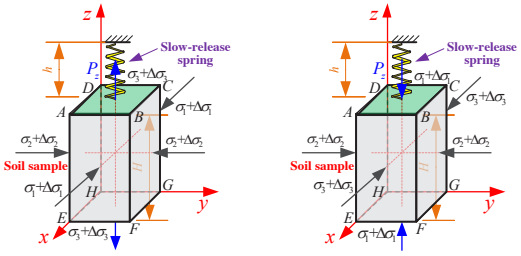

(a) Triaxial tension (b) Triaxial compression

Figure 3. Schematic diagram of numerical implementation of the triaxial constant mean effective stress test

The soil sample's strain ε_{z1} and the slow-release spring's strain ε_{z2} are calculated, respectively, as follows:

$$\varepsilon_{z1}=-u_z/H,\quad \varepsilon_{z2}=u_z/h,\quad \varepsilon_{z2}/\varepsilon_{z1}=-H/h \tag{8}$$

where the strain ε_{z1} and ε_{z2} are positive under compression and negative under tension. The stress σ_s of the slow-release spring is given as

$$\sigma_s = E\varepsilon_{z2} \tag{9}$$

The z-axial stress increment $\Delta\sigma_z$ of the soil sample can be expressed as

$$\Delta\sigma_z = \begin{cases} \Delta\sigma_3 = \sigma_s - P_z & \text{for triaxial tension} \\ \Delta\sigma_1 = \sigma_s + P_z & \text{for triaxial compression} \end{cases} \tag{10}$$

where the z-axial loading stress $P_z = P_0 f(t)$. P_0 is a given constant and $f(t)=t/T$ is a linear function of run time t, ranging from 0 to 1. T is the total time of an analysis step of the finite element model. When the analysis step is completed, $t=T$.

Referring to Figure 3, a finite element model is proposed to simulate the triaxial constant mean effective stress test by ABAQUS, as shown in Figure 4, where a slow-release elastic body is instead of the previous slow-release spring to facilitate modeling and improve the convergence of the finite element model, and this elastic body is orthotropic with the modulus of elasticity along the z-direction being E_s=1000kPa, and that one along the x and y direction both being 0.001kPa. The elastic body is a cube with its height h =1 being one standard unit, and the soil sample is a cuboid with its height H=2 being two standard units.

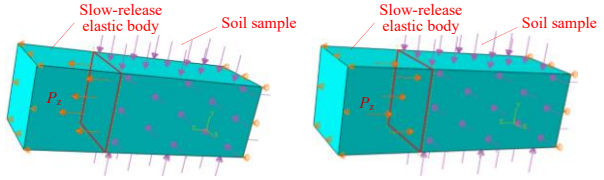

(a) Triaxial tension (b) Triaxial compression

Figure 4. Finite element model of true triaxial constant mean effective stress test.

The displacement and load boundary conditions of the finite element model can also be seen in Figure 4. The initial confining pressure of the soil sample adopts a constant pressure, i.e, $\sigma_x=\sigma_y=\sigma_z=\sigma_m$. The z-axial stress P_z is set as a linear increase in compressive stress from 0 to P_0. The setting of confining pressure increment $\Delta\sigma_x$ and $\Delta\sigma_y$ is the key to simulate the triaxial constant mean effective stress test, where User Subroutine DLOAD is employed to control the confining pressure increment according to Eq. (6) or (7) in each increment of the analysis step. In the User Subroutine DLOAD, an external file (for example, the file is named 'P3.dat') needs to be specified to provide the strain $\varepsilon_{z1}^{(n-1)}$ (or displacement $u_z^{(n-1)}$) and stress $\sigma_x^{(n-1)}$, $\sigma_y^{(n-1)}$, and $\sigma_z^{(n-1)}$ of the soil sample in the last increment, and the stress increment $\Delta\sigma_z^{(n)}$ in the current increment is given as

$$\Delta\sigma_z^{(n)} = \begin{cases} -EH\varepsilon_{z1}^{(n-1)}/h - P_z^{(n)} & \text{for triaxial tension} \\ -EH\varepsilon_{z1}^{(n-1)}/h + P_z^{(n)} & \text{for triaxial compression} \end{cases} \tag{11}$$

When n=1, $\varepsilon_{z1}^{(0)}=0$, $u_z^{(0)}=0$; $\sigma_x^{(0)}=\sigma_y^{(0)}=\sigma_z^{(0)}=\sigma_m$. According to Eq. (6) or (7), the confining pressure increment $\Delta\sigma_x^{(n)}$ and $\Delta\sigma_y^{(n)}$ in current increment can be expressed as

$$\begin{cases} \Delta\sigma_x^{(n)} = B_1 \cdot \Delta\sigma_z^{(n)} \\ \Delta\sigma_y^{(n)} = B_2 \cdot \Delta\sigma_z^{(n)} \end{cases} \tag{12}$$

The return values $\Delta\sigma_x^{(n)}$ and $\Delta\sigma_y^{(n)}$ of User Subroutine DLOAD can be determined by Eq. (12), and these return values will be used in the finite element calculation of the nth increment. When the calculation of the nth increment is completed, User Subroutine URDFIL is used to extract the element stress and strain information in this increment, and then the strain $\varepsilon_{z1}^{(n)}$ and stress $\sigma_x^{(n)}$, $\sigma_y^{(n)}$, and $\sigma_z^{(n)}$ of the soil sample in the current increment will be written to the previous external file by two Utility Subroutines, POSFIL, and DBFILE. In the next increment, the updated strain $\varepsilon_{z1}^{(n)}$ and $\sigma_x^{(n)}$, $\sigma_y^{(n)}$, and $\sigma_z^{(n)}$ of the soil sample in the external file is used again by User Subroutine DLOAD, and so on.

The finite element simulation based on ABAQUS adopts two analysis steps: (1) the GeoStatic analysis step is used to simulate the initial geo stress equilibrium and isostatic consolidation; (2) the General Static analysis step with 1000 fixed increments is used to simulate triaxial compression or triaxial tension with constant mean effective stress.

3 DEMONSTRATION EXAMPLES

3.1 *Mohr-Coulomb model*

To verify the reliability of the above method in the simulation of true triaxial constant mean effective stress test of a soil sample, the Mohr-Coulomb model is adopted to observe its preformation by showing its yield surface on the π plane and other specified stress paths. Material parameters of the Mohr-Coulomb model are shown in Table 2, where E is elasticity modulus, v is Poisson's ratio, φ is internal friction angle, and Ψ is dilatancy angle. During the simulation of true triaxial constant mean effective stress test, the initial confining pressure σ_m= 200kPa; the corresponding P_0=800kPa for triaxial tension, and P_0=300kPa for triaxial compression.

Table 2. Material parameters of Mohr-Coulomb model

Material parameters	E (MPa)	v	φ (°)	Ψ (°)	c (kPa)
Soil sample	80	0.35	45	45	0

Each set of B_1 and B_2 selected from Table 1 will ensure that the soil samples are loaded along the specified stress paths of thirteen kinds of Lode's angles, respectively, which are adopted in the finite element model of true triaxial constant mean effective stress test. So thirteen groups of stress-strain and volume variation curves of soil samples can be calculated according to the specified Lode's angle. However, only six groups of curves corresponding to six kinds of Lode's angles are plotted to make the figure clearer in Figure 5 (a) and (c).

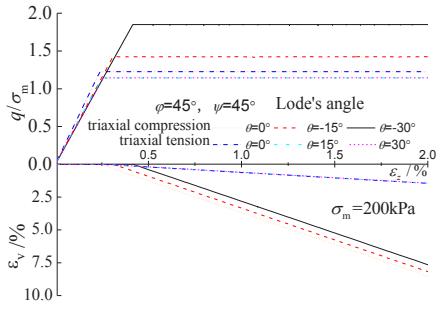

(a) stress ratio & volumetric strain

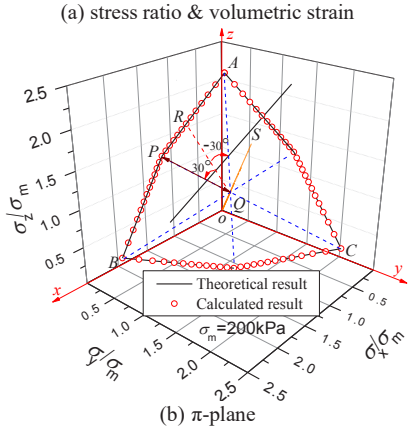

(b) π-plane

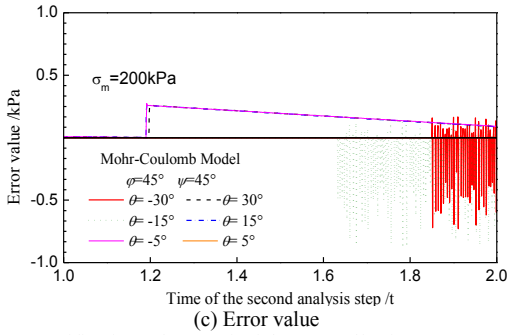

(c) Error value

Figure 5. Verification of true triaxial mean effective stress numerical simulation by using the Mohr-Coulomb model.

Figure 5 (a) shows that the complete stress ratio q/σ_m-axial strain ε_z curves and the volumetric strain ε_v-ε_z curves of soil samples can all be obtained from true triaxial mean effective stress numerical simulation even after the deviatoric stress q of the soil samples reach their yield strength. According to the specified Lode's angle, the stress point $P(\sigma_x, \sigma_y, \sigma_z)$ of the soil sample, which is at the state of its deviatoric stress q reaching to the yield strength, can be employed to obtain the yield surface on π plane as shown in Figure 5 (b). In this figure, Points P, R, and A represent the three yield state stress points of the Mohr-Coulomb model on π plane with Lode's angle θ=30˚, 0˚, and -30˚, respectively. There are eleven other similar calculated data points between Points P and A, which are all obtained from the simulation of true triaxial mean effective stress test of a soil sample loaded along the specified stress paths of different Lode's angles. Since these yield state stress points on the π plane are axisymmetrically distributed along with six 60-degree phase angles, the spatial positions of 72 yield state stress points can also be determined to plot the complete yield surface of the Mohr-Coulomb model. It can be found that the yield surface obtained by the FEM calculation is in perfect agreement with the theoretical result of the Mohr-Coulomb model. During the simulation of the true triaxial constant mean effective stress test, the error value between the mean effective stress and the specified value of 200kPa in each increment is shown in Figure 5 (c). It shows that the error stress is controlled within 1kPa, and the proposed calculation method is stable and reliable.

3.2 *Other classical yield criteria model*

To verify the applicability of the proposed method to other classical yield criterion models, the Matsuoka-Nakai model, Lade-Duncan model, and Drucker-Prager model are adopted in the finite element model of true triaxial constant mean effective stress test, respectively. The yield criteria function of these three classical models are given as follow:

$$\begin{cases} I_1 I_2 / I_3 = (9-\sin^2\varphi)/(1-\sin^2\varphi) & \text{for Matsuoka-Nakai} \\ I_1^3 / I_3 = (3-\sin\varphi)^3/[(1-\sin\varphi)\cos^2\varphi] & \text{for Lade-Duncan} \\ q - 2I_1\sin\varphi/(3-\sin\varphi) = 0 & \text{for Drucker-Prager} \end{cases} \quad (13)$$

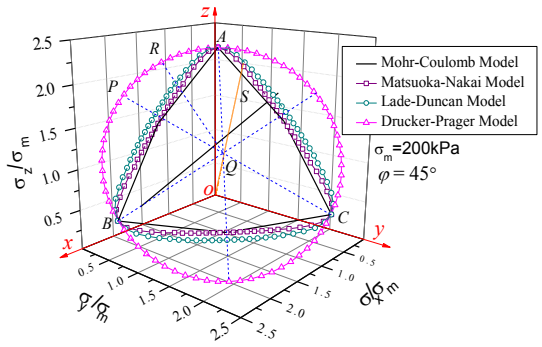

Figure 6. Yield surface of classical yield criteria model on π plane by true triaxial mean effective stress numerical simulation

Where I_2 and I_3 are the second and third invariants of the effective stress tensor, respectively. When the material parameters of these three classical models are the same as the Mohr-Coulomb model, their yield surface on the π plane can also be obtained by the proposed calculation method in Figure 6. It shows that these yield surfaces obtained by the FEM calculation are also in perfect agreement with the theoretical curves according to Eq. (13).

3.3 *Strain-softening model*

To verify the applicability of the proposed method to the strain-softening model, an elasto-viscoplastic model (Wang et al., 2016) based on super-subloading yield surface is also adopted in the simulation of true triaxial constant mean effective stress test. Material parameters of this model are shown in Table 3, where v is also Poisson's ratio; e_0 is the initial void ratio; M is the critical state stress ratio $=6\sin\varphi/(3-\sin\varphi)$; λ and κ are compression index and swelling index; c_0 and m are the coefficients of correlation with the viscosity; α, β, ξ, and ω are the coefficients of structural properties and overconsolidation of soil. The result of the numerical simulation is given in Figure 7. It shows that the yield surface of the strain-softening model from peak strength to residual strength can all be correctly calculated to obtain their yield locus on the π plane.

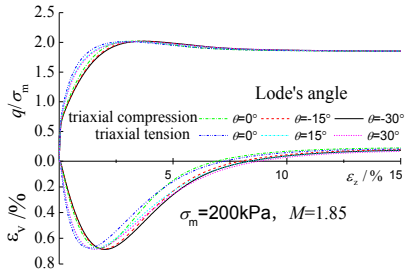

(a) stress ratio & volumetric strain

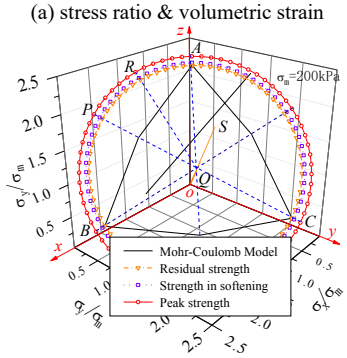

(b) π-plane

Figure 7. Verification of true triaxial mean effective stress numerical simulation by Strain softening model.

Table 3. Material parameters of an elasto-viscoplastic model based on super-subloading yield surface

v	e_0	M	λ	κ	c_0	m	α	β	ξ	ω
0.3	0.72	1.85	0.05	0.0041	1.96×10^9	28.8	0.5	5.0	1.0	1.8

4 CONCLUSIONS

Based on ABAQUS, a simple method is proposed to realize the FEM simulation of a true triaxial constant mean effective stress test by two User Subroutines DLOAD, and URDFILas well as two Utility Subroutines, POSFIL, and DBFILE.

This new method has been tested to observe the performance of five kinds of soil models on the π plane, which yield surfaces obtained by the FEM calculation are in perfect agreement with the theoretical results.

The new method has shown a stable convergence and high precision and provides a practical way for strain hardening, strain softening, elastoplastic, elasto-viscoplastic, and other complex models.

5 ACKNOWLEDGEMENTS

The research has been funded by the Excellent Youth Project of the Research Foundation of Education Bureau of Hunan Province (17B260), High-level Talent Gathering Project in Hunan Province (2019RS1059), and State Foundation for Studying Abroad (201908430091).

6 REFERENCES

Hashiguchi K. and Chen Z. P. 1998. Elasto-plastic constitutive equations of soils with the subloading surface and the rotational hardening. *Int. J. Numer. Anal. Meth. And Geomech.*, 22, 197-227. Lagioia R. and Panteghini A. 2016. On the existence of a unique class of yield and failure criteria comprising Tresca, von Mises, Drucker-Prager, Mohr-Coulomb, Galileo–Rankine, Matsuoka-Nakai and Lade-Duncan. *Proceedings of the Royal Society A: Mathematical, Physical and Engineering Sciences*, 472(2185): 1-21.

Nakai T., Matsuoka H., et al. 1986. True triaxial tests on normally consolidated clay and analysis of the observed shear behavior using elastoplastic constitutive models. *Soils and Foundations*, 26(4): 67-78.

Tasiopoulou P. and Gerolymos N. 2016. Constitutive modelling of sand: a progressive calibration procedure accounting for intrinsic and stress-induced anisotropy. *Géotechnique*, 66(9): 754-770.

Wheeler S.J., Anu N. M. K., and Matti L. 2003. An anisotropic elastoplastic model for soft clays. *Canadian Geotechnical Journal*, 40(2): 403-418.

Wang Z.C., Jiang M. J., et al. 2016. An elasto-viscoplastic constitutive model and its stress integration algorithm based on super-subloading yield surface. *Rock and Soil Mechanics*,37(2): 357-366. (In Chinese)